Electroencephalography and Clinical Neurophysiology, 1981, 51: 306–327

ON THE CURRENTS THAT FLOW DURING THE STRYCHNINE SPIKE [1]

A.L. TOWE, M.D. MANN and G.W. HARDING

Department of Physiology and Biophysics, University of Washington School of Medicine, Seattle, Wash. 98195 (U.S.A.)

(Accepted for publication: October 2, 1980)

Pericruciate cortex is of special interest in that it contains pyramidal tract neurons and comprises electrically excitable motor cortex. Though much of this cortex — cytoarchitectonic fields 4γ (Hassler and Muhs-Clement 1964) — is buried within the cruciate sulcus, a large portion is accessible to study on the free gyral surface on either side of the sulcus. The lateral region is topographically related to the contralateral forepaw and contains neurons which, under chloralose anesthesia, show a variety of cutaneous excitatory receptive fields, including small contralateral fields, medium bilateral fields and fields that include the entire body surface. These receptive fields cluster into at least 3 distinct groups, described as small-field, bilateral-field and wide-field (also bilateral). When recording from neurons in this cortex, the receptive fields may be characterized with a brief electrical pulse to the central footpad of each limb. When characterized in this manner, the terms *sa*, *sb*, and *m* neurons may be used, according to their patterns of responsiveness (Towe et al. 1968, 1976; Nyquist and Towe 1970). The small-field, or *sa*, neurons are concentrated in layers II and III, whereas the wide-field, or *m*, neurons are concentrated in layers IIIc, V and VI. About half of the *m* neurons send their axons down the medullary pyramids, and about 80% of the pyramidal tract neurons are *m* neurons (Towe et al. 1968, 1976). The bilateral-field, or *sb*, neurons, on the other hand, are scattered throughout the depth of the cortex, primarily anterior to the cruciate sulcus (Towe et al. 1968; Nyquist and Towe 1970), and depend upon the opposite cerebral hemisphere for their ipsilateral cutaneous responsiveness (Tyner and Towe 1970). The size of a wide-field neuron's excitatory receptive field is state-dependent (Baker et al. 1971). Under pentobarbital anesthesia, *m* neurons fail to respond to any form of cutaneous stimulation (Harding et al. 1979). Nonetheless, strychnine spikes may be produced in this tissue under either chloralose or pentobarbital anesthesia.

It has recently been shown in chloralose-anesthetized cats that topically applied strychnine sulfate immediately and profoundly enhances the responsiveness of *sa* and *sb* neurons to cutaneous stimulation (Towe and Mann 1973; Mann and Towe 1974). The *m* neurons in postcruciate tissue respond to stimulation anywhere on the body surface except for the topographically 'on-focus' skin

[1] This work was supported by USPHS Research Grants NS00396 and NS05136 from the National Institute of Neurological and Communicative Disorders and Stroke. Dr. Mann's present address is: Department of Physiology and Biophysics, University of Nebraska Medical Center, Omaha, Nebr. 68105, U.S.A.

Abbreviations: EPSP = excitatory postsynaptic potential; IPSP = inhibitory postsynaptic potential; PDS = paroxysmal depolarization shift; *sa* neuron = responds only to stimulation of the contralateral forepaw; *sb* neuron = responds to stimulation of each forepaw; *m* neuron = responds to stimulation of each of the 4 paws; SI = somatosensory area I.

site as though no strychnine were present. The enhancement of *m* neuron responsiveness to on-focus stimulation can be understood in terms of the known excitatory action of *sa* neurons onto *m* neurons (Towe et al. 1968, 1976); the *m* neurons are only indirectly affected by topical strychnine, through the increased activity of the affected *sa* neurons. It was suggested (Mann and Towe 1974) that because the *sa* neurons are largely responsible for the primary evoked response (Amassian et al. 1964; Towe 1966) and are directly affected by topical strychnine, they may also be largely responsible for the strychnine spike. The *sa* neurons discharge in a fixed temporal relation to both 'off-focus' and 'spontaneous' strychnine spikes, whereas the *m* neuron discharges vary in their temporal relation to such events (Mann and Towe 1974).

In studying the pattern of net vertical current flow through depth in the postcruciate cortex during the primary evoked response, Towe (1966) [2] found that about 80% of the current flow could be ascribed to the *sa* neurons. If these neurons are similarly involved during the strychnine spike, then the pattern of net vertical current and transmembrane current flows might be amplified and temporally extended versions of those observed during the normal primary evoked response. These current flows have been measured and are described in this paper. A mechanism for the production of the strychnine spike after topical application is also proposed in terms of our current understanding of neuronal circuitry within postcruciate field 4γ tissue. Both focal and generalized convulsive activity are discussed within the framework of this mechanism.

Methods

Domestic cats were anesthetized with alpha-chloralose (60 mg/kg, intraperitoneally) and paralyzed with decamethonium bromide (1—2 mg/h, intravenously). Bilateral pneumothorax and cisternal drainage via the atlanto-occipital membrane were produced to reduce cerebral pulsations, and the animals were ventilated at 17—20 strokes/min with 30—40 ml/stroke, against an expiratory pressure of 3.5 cm of water. The right frontal cranium was removed to expose the pericruciate cortex, and the cortex was covered with a protective polyethylene sheet soon after the dura mater was reflected. This sheet was removed during recording sessions. Rectal temperature was maintained at 38°C by an abdominal DC heating pad under servocontrol by a thermoprobe. Bipolar needle electrodes were inserted into the central footpad of each forepaw, and square pulse stimuli of 0.1 msec duration and supramaximal strength (30 mA) were delivered. A silver ball electrode monitored the cortical surface evoked response while a 2.5 M NaCl-filled micropipette of 2—4 μm tip diameter simultaneously recorded the response at different depths in the cortex. The microelectrode was advanced in 0.1 mm steps to a depth of 2 3 mm, and 10 records were taken for each input at each depth. Upon completion of the first penetration, the microelectrode either was left in place or was withdrawn to the cortical surface, and a drop of 0.2% strychnine sulfate solution was extruded from a 22-gauge needle onto the microelectrode shaft and thence onto the cerebral surface. After full development of the strychnine effect — 4—6 min — a second set of recordings was taken either by withdrawing or reinserting the electrode in 0.1 mm steps (0.05 mm steps also were used, but were found to be unnecessarily small). Each full series of recordings required 6—12 min to complete, thus spanning or slightly exceeding the period during which the strychnine spike remained at a stable maximum (Towe and Mann 1973; Mann and Towe 1974).

Recordings were taken in two ways, one using the rapid data acquisition system (Morse 1963) and the other being fully computer-

[2] The graphs of Figs. 3 and 4 of that paper are interchanged and placed above the wrong legends.

automated (Harding and Towe 1976). In the former mode, all stimuli were delivered via radio-frequency isolation transformers. The recording microelectrode was coupled through a cathode follower stage to a Grass P5 preamplifier, set at 0.7 Hz and 10 kHz half-amplitude bandpass. The output of the preamplifier was led to a Philbrick differential amplifier of the data acquisition system. The surface-monitoring electrode was similarly arranged, with the cathode follower input stage. Following each stimulus, a 100 msec record was digitized at 2.5 kHz per channel, through a 25 nsec aperture, with a 6-bit amplitude accuracy, and was written on magnetic tape for subsequent processing. In the fully automated mode, all stimuli were delivered via infrared photon-coupled diode pairs, for isolation from ground, and the recording microelectrode was coupled through a FET voltage follower to a Grass P5 preamplifier, set at 0.1 Hz and 10 kHz half-amplitude bandpass. The output of the preamplifier was led to a 10-bit A/D converter coupled to a Raytheon PB440 computer. The surface-monitoring electrode was similarly arranged, without the FET input stage. Following each stimulus, an 85 msec record was digitized at 1.0 kHz per channel, through a 1.0 μsec/bit tracking converter, and read directly into memory for subsequent processing.

The patterns of voltage change at different depths in the cortex through time after the stimulus were obtained by averaging 4—8 records for each input and assembling the resulting array into a time-depth surface. The patterns of net vertical current flow were obtained from this array in the manner described previously (Towe 1966). In a strict sense, a Laplacian electrode arrangement should be used to obtain the appropriate voltage and conductance measurements. Also, the measurements should be taken simultaneously at all the sample points during a single event. However, the compromise method employed in this study — averaging repeated measurements at each sample point along a single line normal to the laminae of the cerebral cortex — should yield an approximately correct picture, for the following reasons: the cerebral cortex is probably much like frog cerebellum (Nicholson and Freeman 1975) in being a relatively homogeneous, anisotropic, ohmic medium. Furthermore, the cutaneous stimulus evokes relatively synchronous activity in a spatially large ensemble of neurons, and the event is essentially stationary after a short, initial transient at the iterative stimulus rate of 1/sec. This allows one-dimensional analysis. Hoeltzell and Dykes (1979) found area 3b of cat posterior sigmoid gyrus to be anisotropic, with high anteroposterior conductivity (σ_x) in layers II and III, and high mediolateral conductivity (σ_y) in layer IV. Except in layer I, conductivity normal to the laminae (σ_z) — what we call the vertical axis — is nearly uniform, being only 10% lower in layer IV than above and below that lamina. As in frog cerebellum (Nicholson and Freeman 1975), this cerebral region appeared to be homogeneous over short distances (1—2 mm). Measurements of the possible dependence of conductivity on the magnitude of the evoked potential were not made by Hoeltzell and Dykes (1979), but Nicholson and Freeman (1975) found a negligible dependence in frog cerebellum, supporting the notion of an ohmic medium. In their study of current source density (CSD), the latter authors state that: 'As the diameter of the population increases, the resemblance between the single second derivative and the CSD increases, but a large synchronous ensemble is necessary in order to obtain close similarity.' Our own experience with postcruciate forepaw tissue strongly suggests that this condition is true, and that the event is the same on repeated trials. Thus, the one-dimensional method followed here, with

$$J_z(t) = -\sigma_z \frac{\partial \phi(t)}{\partial z} \text{ and } i_m(t) = -\sigma_z \frac{\partial^2 \phi(t)}{\partial z^2}$$

(where J_z is net vertical current flow, i_m is net transmembrane current flow, and ϕ is the field potential), should yield sufficiently accurate results.

Results

The specific configuration of the primary response and the strychnine spike evoked by cutaneous stimulation and recorded at the pial surface and through depth in the cerebral cortex varied among animals and among recording sites — though not over short distances. However, the patterns of net vertical current flow [J(z,t)] were rather similar among animals and among recording sites. We did not obtain enough information to determine whether minor differences in these patterns were uniquely associated with the specific pattern of 'reversal' of the primary response in depth. There are 3 general patterns of such 'reversal,' two of which are illustrated in Fig. 1A. Each trace in the figure is the average of the 4 most similar traces — in general, identical — among the last 6 in a block of 10 responses, using a 1/sec, supramaximal shock to the central footpad of the contralateral forepaw. This eliminated the small transient response detectable in the second and third responses to a 1/sec train of stimuli. A block of 10 responses was recorded at each successive 0.1 mm interval in depth, from the pial surface (bottom trace in each figure) to 2.0—2.4 mm deep, and the averages were assembled to form a voltage surface. Fig. $1A_1$ shows a common pattern of 'reversal' in which the surface-positive component

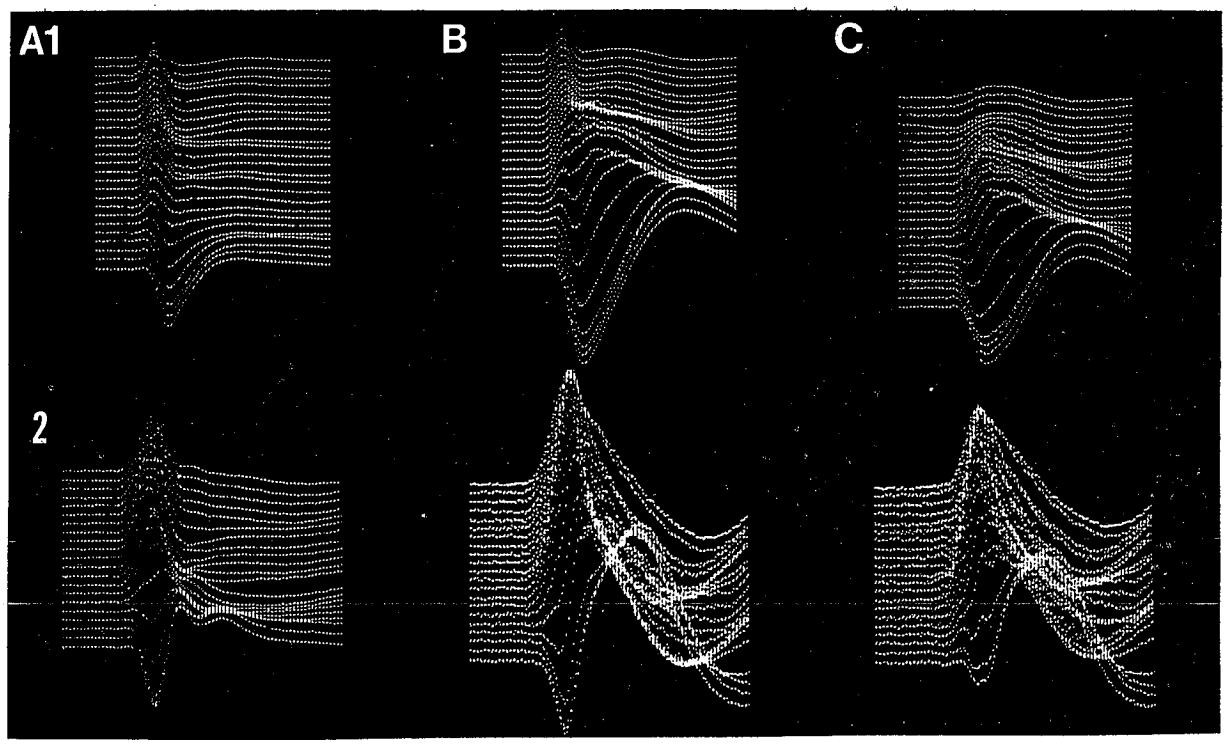

Fig. 1. Strychnine spikes and primary evoked responses to contralateral forepaw stimulation at 1/sec recorded at 0.1 mm depth intervals in the postcruciate forepaw focus in two different preparations (rows 1 and 2). Responses at the pial surface are shown in the bottom trace and the deepest recording in the top trace of each set (maximal depths: 2.4 mm in row 1, 2.0 mm in row 2). A: two different patterns of 'reversal' of control primary responses in depth. B: voltage surfaces for the strychnine spike recorded in the same microelectrode tracks as in A. C: strychnine-minus-control surface constructed by time-point-by-point subtraction of the primary response at each depth in A from the strychnine spike at each depth in B. Total sweep duration: 60 msec in row 1; 45 msec in row 2. The initial positivity of surface-recorded response in A_1 is about 4 mV; same calibration applies to all records.

rapidly diminishes with depth as an early negative component appears, often seeming to 'push' the positive component later in time. In this pattern, a specific depth of 'reversal' cannot be specified. Fig. $1A_2$ shows another common pattern, in which the surface-positive/negative components rapidly diminish with depth to nearly zero and then reappear in the reverse order below that depth. In this pattern, a 'reversal' depth — about 0.4 mm in this illustration — can be specified. However, it should be noted that the 'reversal' in depth never yields a mirror image of the surface configuration.

Another less common pattern yields no specific depth of 'reversal,' because the negative component of the surface-positive/negative configuration simply moves progressively earlier in time, overriding and thus removing the positive component. A later positive component usually develops such that below about 0.4 mm a negative-positive configuration prevails. In the discussion that follows, these different 'reversal' patterns will be treated as a single event, the variable of interest being the pattern of voltage that is added as a consequence of topical strychnine application to the recording site.

The marked enhancement of the primary evoked response after strychnine application is well documented; Fig. 1B shows the effects as seen throughout the depth of the cortex. As with surface recording, there is a marked enhancement of the primary response, especially in the upper half of the cortex, along with the appearance of a later negativity through most of the cortex. Subtracting the normal primary response traces in A from the strychnine spike traces in B yields the pattern of added voltage shown in C of Fig. 1. It is apparent that a large positive-negative component is added in the upper half of the cortex and a smaller negative component is added in the lower half. The large negative component added in Fig. $1C_2$ was seen in only a few penetrations, and may relate to the amount of strychnine applied and to the condition of the pia mater at the site of application.

Fig. 1 reveals a characteristic common to both the primary response and the strychnine spike: in the upper half of the cortex, excluding layer I, the peak positivity shifts progressively with an apparent upward movement of 0.10 m/sec. This is the same velocity as the apparent upward spread of neuronal activity from deep layer III through layer II after cutaneous stimulation in normal (anesthetized) animals (Amassian et al. 1964; Towe et al. 1964; Towe 1966). On the other hand, the later negativity that is added after topical strychnine (Fig. 1B and C) sweeps upward at only 0.02 m/sec over the same depth interval. Thus, the strychnine effect may involve two distinct processes: an enhancement of normal activity and the addition of new, abnormal activity.

Ipsilateral responses

In postcruciate tissue, the strychnine spike appears only after stimulation of the topographically related, contralateral input site — unless a large amount of strychnine is applied (Towe and Mann 1973). Clear and repeatable responses can regularly be evoked by stimulation of any cutaneous site in chloralose-anesthetized cats (Towe et al. 1964; Towe 1966; Towe and Mann 1973), yet with the exception of the classical primary response, these responses are not affected by topical strychnine (Towe and Mann 1973). Even after a large amount of strychnine is applied, the strychnine spikes that develop to 'off-focus' stimulation are clearly added to the normal responses, at widely varying latencies on repeated trials (Towe and Mann 1973). These same phenomena can be seen at the single neuron level: many neurons, including most pyramidal tract neurons, respond to cutaneous stimulation anywhere over the body surface (Towe et al. 1964, 1968, 1976), yet only their responses to stimulation at the topographically related site are enhanced by topical strychnine (Mann and Towe 1974). Thus, it was not surprising to find that the pattern of voltage through depth observed after stimulation of any 'off-focus' site, including ipsilat-

eral sites, did not change after strychnine application. Subtraction of off-focus voltage surfaces taken before and after topical strychnine treatment in every case yielded a flat surface. It follows that the topical strychnine effect does not involve the synapses that are activated by 'off-focus' stimulation; these same synapses appear to be activated by stimulation of the topographically related site.

Alternation phenomenon

After application of strychnine to postcruciate forepaw tissue, iterative stimulation of the contralateral forepaw at 1/sec evokes a strychnine spike in response to each stimulus, the spikes being identical on repeated trials. However, as with topical bicuculline (Harris and Towe 1976), iterative stimulation at 3—4/sec usually results in the appearance of a strychnine spike after every other stimulus, alternating with a slightly-larger-than-normal primary response. This phenomenon is shown in Fig. $2A_1$ by a sequence of surface-recorded responses to contralateral forepaw stimulation at 4/sec; the alternation in response amplitude and configuration is obvious. Fig. $2B_1$ shows

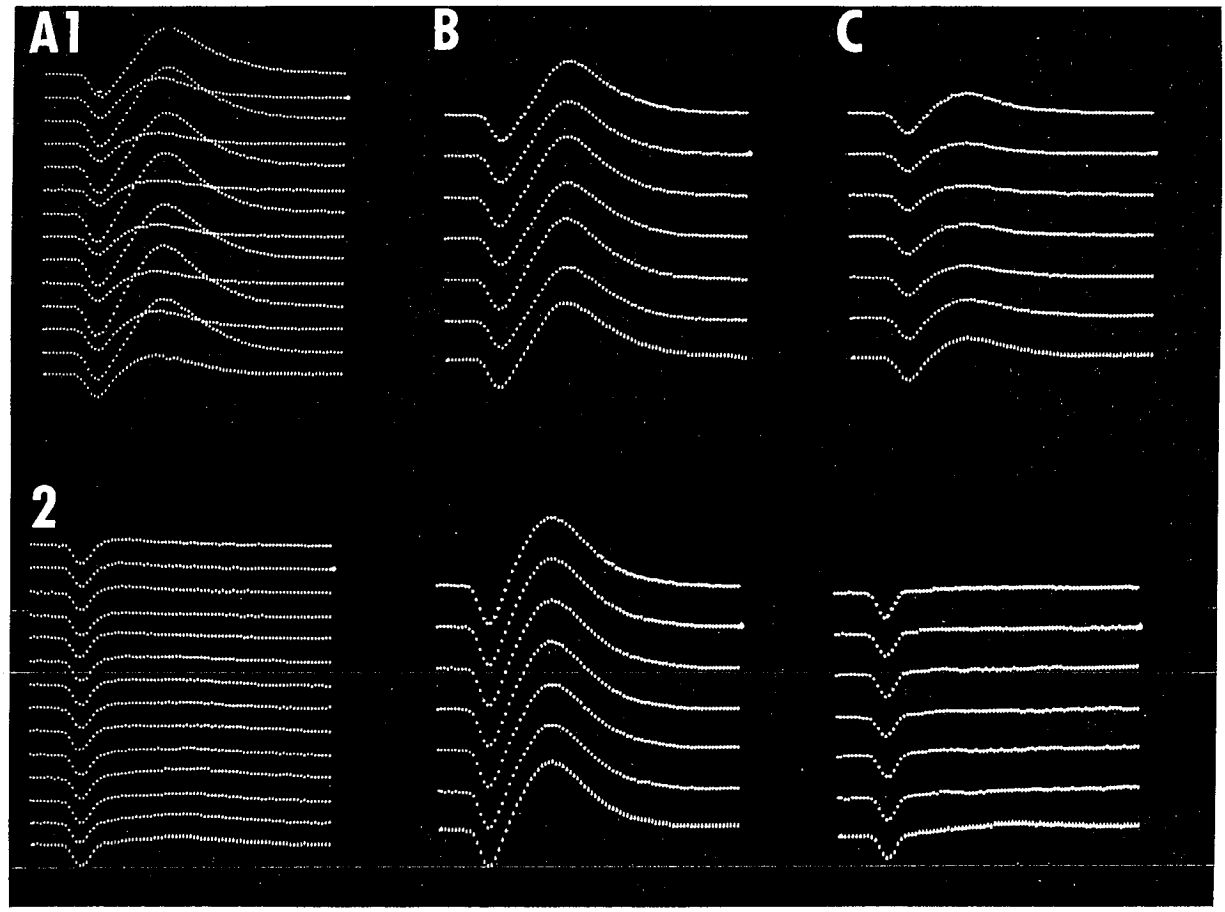

Fig. 2. Consecutive surface-recorded responses to stimulation of the contralateral forepaw at 4/sec (A_1, A_2) and 1/sec (B_2, C_2). A_1: consecutive strychnine spikes, 4/sec. B_1: odd-numbered traces (starting at the top) reproduced from records in A_1. C_1: even-numbered traces reproduced from records in A_1. A_2: primary evoked responses in normal cortex, 4/sec. B_2: consecutive strychnine spikes, 1/sec. C_2: primary response in normal cortex, 1/sec. Total sweep duration: 84 msec. Peak-to-peak voltage is 2 mV in A_2; same calibration in all records.

the alternate responses from Fig. $2A_1$ that almost match the strychnine spikes evoked by 1/sec stimulation (Fig. $2B_2$). Fig. $2C_1$ shows the complementary alternate responses from Fig. $2A_1$ that are similar to the prestrychnine primary responses evoked by 1/sec (Fig. $2C_2$) and 4/sec (Fig. $2A_2$) stimulation. The smaller strychnine spikes during the alternation phenomenon (compare the responses in B_1 with those in B_2 of Fig. 2) may result from a conditioning interaction that occurs over the 250 msec interstimulus interval. The larger primary responses during the alternation phenomenon (compare the responses of C_1 with those of C_2 and A_2 in Fig. 2) suggest again that two distinct processes in the strychnine

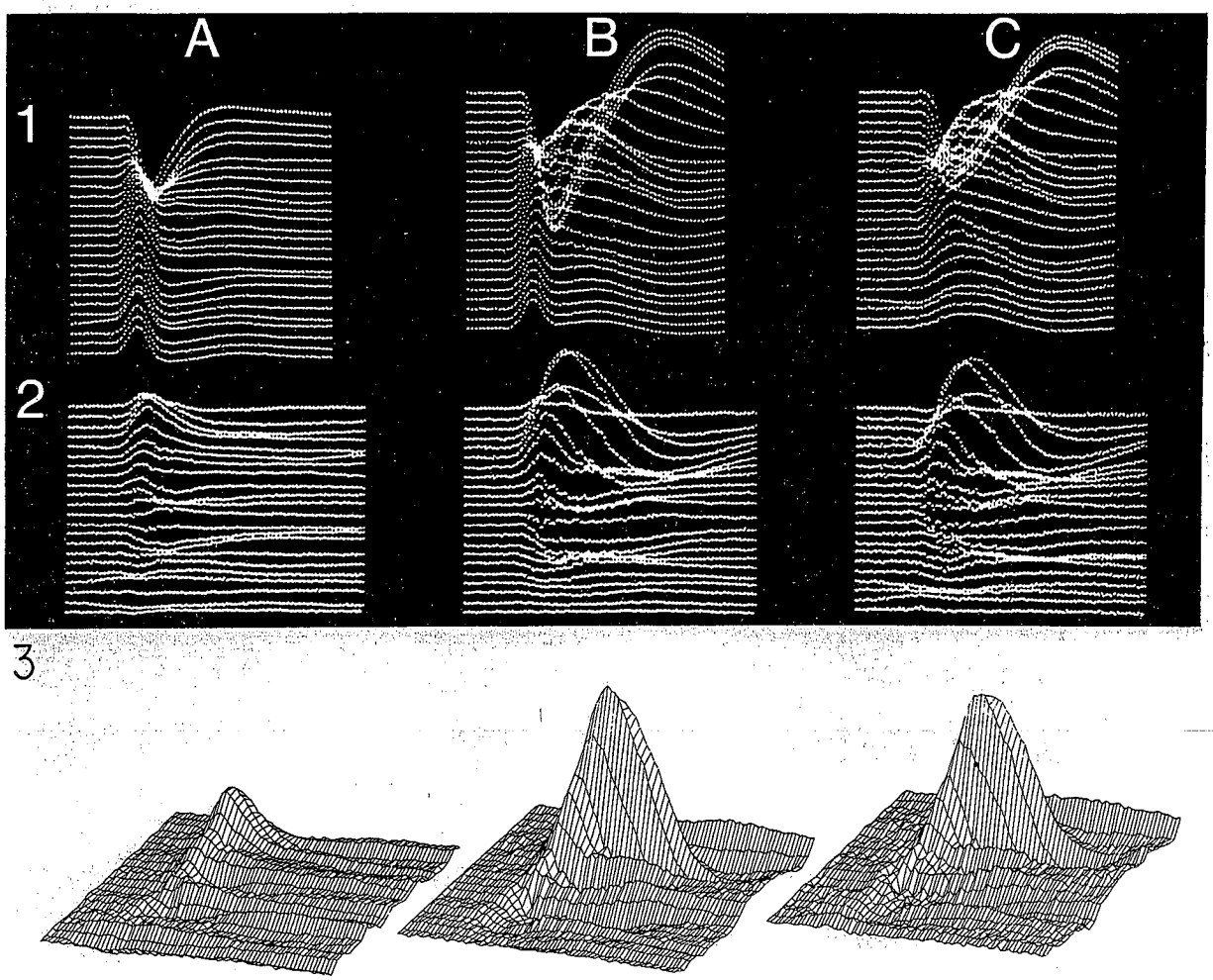

Fig. 3. Voltage stacks and current surfaces for normal (A) and strychnine (B) responses to contralateral forepaw stimulation at 1/sec and strychnine-minus-control differences in C. Row 1: same records as in Fig. 1, row 1 except reversed orientation to show surface records at top, depth increasing downwards. Time reads left to right. Row 2: current traces generated by subtracting voltage records over 0.2 mm intervals in stacks of row 1, placing difference trace at midpoint of interval. Upward deflections indicate net downward current. Row 3: three-dimensional display of the current traces shown in row 2. Upward deflection corresponds to net downward current. Time reads left to right (0—68 msec); depth, top to bottom (first record corresponds to 0.1 mm depth). Total sweep: 60 msec in row 1; 68 msec in row 2. Surface-recorded positivity is about 4 mV in A_1; fourth trace, downward current is about 250 $\mu A/cm^2$ in A_2; and peak current is about 250 $\mu A/cm^2$ in A_3.

effect may be separated at this iterative stimulus rate: the enhanced, normally active process seems to occur after every stimulus, whereas the new, not-normally-active process occurs after every other stimulus. The latter process may have a lengthy refractory or unresponsive period.

Net vertical current flow

During an EPSP, extracellular current flows from other parts of the neuron into the region of active depolarization. The extracellular currents around neighboring, simultaneously active neurons add algebraically, whether EPSPs, IPSPs or both are involved. Thus, for any given pattern of neuronal activity and membrane polarization change, a unique pattern of extracellular current flow is established. Because vertical organization seems to predominate in cerebral tissue, the major component of net current flow at any extracellular point, when resolved in the x, y, z coordinates defined in Methods, must be in the vertical (z) direction. Reasons were given in Methods for expecting that a one-dimensional (z-axis) analysis would yield a fairly accurate picture of the pattern of net vertical current flow, J(z, t). The method is illustrated in Fig. 3, where each voltage record $\phi_z(t)$ in A is subtracted from voltage record $\phi_{z-2}(t)$, to obtain the voltage difference traces, $\Delta\phi_z(t) = \phi_{z-2}(t) - \phi_z(t)$, shown in B. Taking conductivity, σ_z, to be constant throughout the cortical layers (see Hoeltzell and Dykes 1979), the difference voltage is taken to be proportional to net vertical current flow, J_z, with an upward deflection of the difference voltage trace signifying net *downward* current flow. This is an approximation to the continuous function

$$J_z(t) = -\sigma_z \frac{\partial \phi(t)}{\partial z}.$$

(It should be noted that the voltage stacks in the top row of Fig. 3 show the same data as in the top row of Fig. 1, with the stacks reversed such that they read from the pial surface downward.) On the assumption of electrical continuity within the cerebral cortex, the traces of $J_z(t)$ in row 2 of Fig. 3 can be taken to define a continuous surface, and plotted as contour diagrams (Fig. 4) or three-dimensional displays (row 3 of Fig. 3). The latter aid in interpreting the contour maps.

The time-depth contour lines of $J_z = 0$ in Fig. 4 are broken with dots, those of $J_z < 0$ (downward current) are solid and those of $J_z > 0$ (upward current) are dashed. The contour lines are spaced at about 50 μA/cm^2 intervals. Time after the stimulus reads to the right in milliseconds and depth below the pial surface, S, reads downward in millimeters. Fig. $4A_1$ shows the normal pattern of current flow during the primary evoked response in considerably more detail than can be surmised from Fig. 3. The major flow, as determined in a previous study (Towe 1966), is downward in layers II and III, 12—24 msec after the forepaw shock; it is 5—6 times larger than the largest net upward flow, which in this preparation developed in the depth interval of layer V (1.3—1.6 mm below the pial surface), 14—28 msec after the forepaw shock. The pattern of current flow during the fully developed, stable strychnine spike, shown in Fig. $4A_2$, shares much in common with the normal pattern, though it is intensified and temporally 'stretched.' The greatest change occurs in layers II and III, where downward net current more than triples and is immediately followed by an intense upward net current that attains its maximum about 0.2 mm deeper in the tissue. The current that is added in the strychnine spike is shown in Fig. $4B_2$, which encodes the difference between the graphs of Figs. $4A_1$ and $4A_2$.

Current flow in relation to cerebral circuitry

Fig. $4B_1$ shows a *highly* schematized diagram of the circuitry involved in the production of the primary evoked response (Towe 1966; Towe et al. 1968, 1976; Slimp and Towe 1980). The major net vertical current flow (J_z), shown in Fig. $4A_1$, is indicated by arrow *a*. Maximal net upward current flow is always smaller and slightly deeper in the tissue. In the case illustrated, it occurs $0.9 < z < 1.2$ mm (arrow *k*) and $1.4 < z < 1.6$ mm

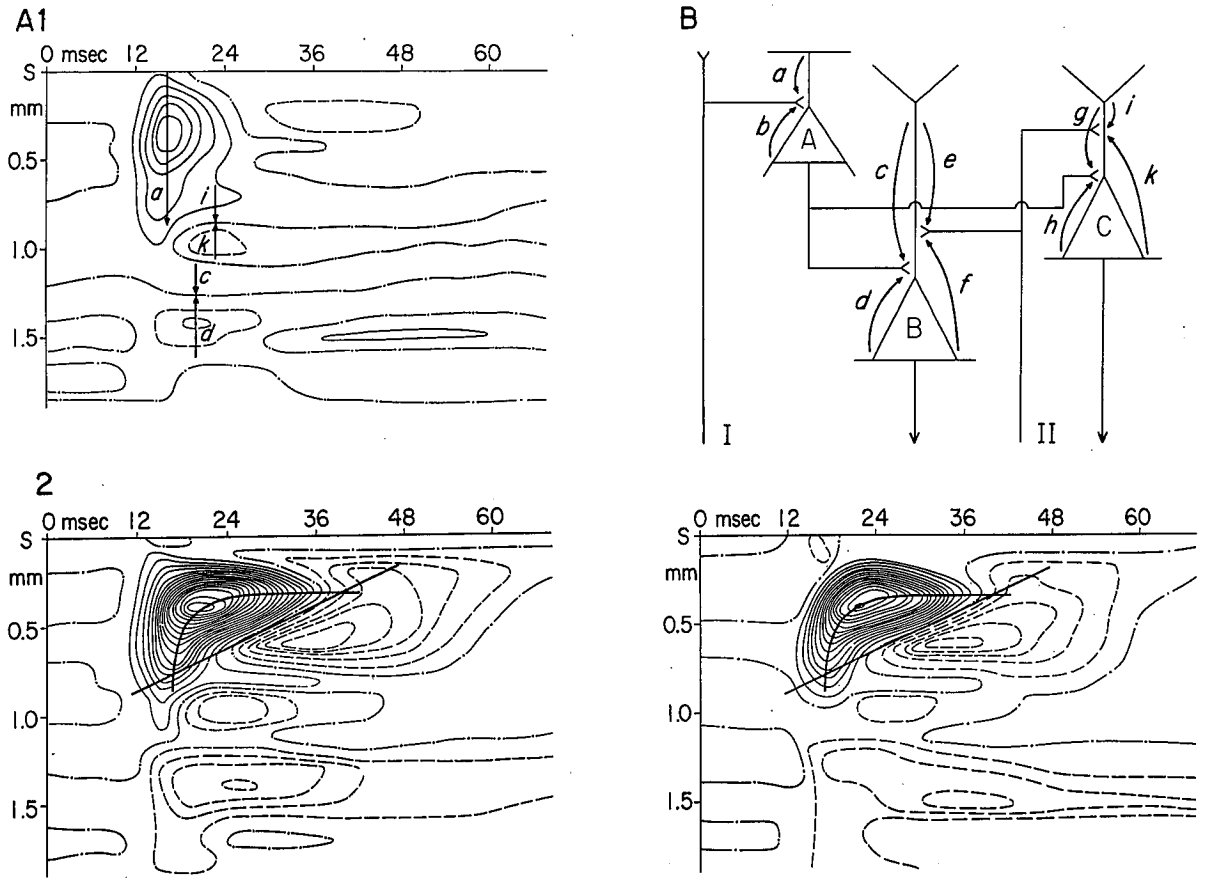

Fig. 4. Current flow contour maps are shown in relation to cerebral circuit diagram (B_1). A_1: primary response evoked in normal cortex by 1/sec stimulation of the contralateral forepaw. A_2: strychnine spike, similarly evoked. B_2: strychnine-minus-control current contour computed for records in A_1 and A_2. Data from same penetrations as in Fig. 3. Same conventions apply. B_1: circuit diagram for postcruciate forepaw focus deduced from single unit studies. Time is encoded in the diagram from left to right and depth from top to bottom. Current flows predicted for activity at synaptic contacts shown in the diagram are indicated by arrows. Corresponding resultant current flows (after cancellation) are indicated by similarly lettered arrows in the contour map of A_1. Heavy, straight lines in A_2 and B_2 are drawn through zero net vertical current contours ($J_z = 0$), while heavy, curved lines follow the ridge of peak net downward current flow.

(arrow *d*) below the pial surface — in layer IIIc and in layer V by the criteria of Hassler and Muhs-Clement (1964). It develops 3—5 msec after the strong downward current (arrow *a*), and diminishes to negligible magnitude 8—12 msec later.

The strong downward current flow may be attributed to EPSPs on small and medium pyramidal-shaped neurons of layers II and III (Amassian et al. 1964; Towe 1966), whereas the smaller net upward flows may be related to EPSPs on medium and large pyramidal-shaped neurons of layer IIIc and of layer V (Towe 1966). The manner in which these currents are produced may be visualized in Fig. $4B_1$, which shows the fairly-well-documented connectivity among the *sa* and *m* neurons within postcruciate field 4γ (Towe et al. 1964, 1968, 1976; Towe and Tyner 1971; Mann and Towe 1974; Harding et al. 1979; Slimp and Towe 1980). Cell A in Fig. $4B_1$ represents the population of *sa* neurons in

layers II and III. Cell B represents the population layer V *m* neurons and cell C that of layer IIIc *m* neurons (Towe et al. 1968, 1976). Thalamocortical input I in Fig. $4B_1$ is activated by stimulation at the topographic focus for the recording site and activates *sa* neurons, which in turn affect the *m* neurons (Towe et al. 1968, 1976; Mann and Towe 1974; Harding et al. 1979; Slimp and Towe 1980). Input II in Fig. $4B_1$ can be activated by stimulation anywhere on the body surface (the pathway yields a longer latency than input I) and affects only the *m* neurons — indeed, it is the excitatory action of this input that defines the neurons as members of the *m* subset (Towe et al. 1968, 1976; Tyner 1975; Satterthwaite et al. 1978; Mann 1979).

The extracellular current flows produced by these synaptic actions are shown by the arrows labeled *a* through *k*; the specific sites of synaptic action are statistical abstractions on populations of distributed synapses. The spatial organization and temporal relationships lead to reduction or cancellation of several currents, such as $b + c + g$, $c + h$ and $e + k$, leaving *a* as a strong net downward flow, along with lesser net upward flows deeper in the tissue, such as *d* and *h*, continuing into *f* and *k*. These net currents are indicated by the labeled arrows in Fig. $4A_1$, along with the incompletely cancelled components *c* and *i* near their depth-time regions of greatest flow. Removal of the currents due to the synaptic actions induced by input I and by cell A in this model yields the pattern of current flow seen after stimulation of topographically 'off-focus' input sites, which activate only input II.

Current flow during the strychnine spike

After topical application of strychnine sulfate to the postcruciate forepaw focus in field 4γ, stimulation of the contralateral forepaw evoked abnormally large net vertical current flows, especially in the upper half of the cortex. As seen in Fig. $4A_2$, current flow began with its normal pattern, but rapidly increased in magnitude and took on a different character in layers II and III. Net upward currents *d* and *k* intensified, in this case by a factor of two, and continued longer than normal. In the depth interval $0.2 < z < 0.8$ mm, net downward current more than tripled in magnitude, becoming especially intense in the depth interval $0.3 < z < 0.6$ mm.

The apparent upward velocity of peak downward current flow as indicated by the average slope from $z = 0.8$ to $z = 0.45$ mm of the heavy curved line in Fig. $4A_2$ was about 0.10 m/sec, whereas the slopes of the iso-current lines between peak downward and peak upward (heavy straight line in Fig. $4A_2$) were all about 0.02 m/sec. This behavior suggests that two processes were involved, one of which spread upward from cell to cell in the usual manner at an average velocity of 0.10 m/sec and the other of which moved upward along individual neurons.

These features also can be seen in Fig. $4B_2$, which maps the current that was added to the normal current flow (Fig. $4A_1$) after the strychnine effect had fully developed (Fig. $4A_2$). Whereas only 50—100 $\mu A/cm^2$ of upward current was added in the lower half of the cortex, fully 750 $\mu A/cm^2$ of downward current and 250 $\mu A/cm^2$ of upward current were added in the upper third of the cortex. Clearly, the major change effected by topically applied strychnine took place in layers II and III of the cortex.

The same behavior is illustrated for another animal in row 1 of Fig. 6. Here, maximal net downward current increased by about 1 mA/cm^2 and maximal net upward current by nearly 750 $\mu A/cm^2$ — both exceedingly large current flows. There was an increase in current flow deeper in the cortex as well, though relatively smaller. Net current flow in the depth interval $1.25 < z < 1.6$ mm was downward rather than upward, a condition seen in several preparations which may relate to cortical thickness and the details of histological structure. It probably corresponds to current *c* of Fig. $4A_1$, current *d* being much weaker in these preparations.

Current flow during the alternation phenomenon

In untreated animals, calculation of J(z,t) from alternate, even-numbered traces in 3—4/sec iterative series of stimuli yields a pattern identical to that calculated from alternate, odd-numbered traces of the same series. In strychnine-treated animals, such a calculation yields two markedly different patterns, one similar to the normal 1/sec and the 3—4/sec pattern observed before the application of strychnine and the other similar to the 1/sec pattern of the strychnine spike. Row 1 of Fig. 5 shows the familiar pattern of J(z,t) recorded in lateral postcruciate tissue after 1/sec stimulation of the contralateral forepaw before (A) and after (B) topical application of strychnine. Prior to the strychnine treatment, 3/sec stimulation yielded the pattern shown in Fig. 5C, which is similar to, but less intense than, that evoked by 1/sec stimulation (Fig. 5A). After strychnine application, clear alternation appeared whenever the iterative stimulus rate was raised to 4/sec. The two patterns of J(z,t) made up from alternate traces are shown in Fig. 5D and E. The general similarity of the 'small half' of the alternation series (Fig. 5D) to the 3/sec control pattern (Fig. 5C) is obvious. The two sets of measurements were taken on two separate microelectrode penetrations through nominally the same track, so the depth values may not agree exactly. The major difference was found in the prolongation of net downward

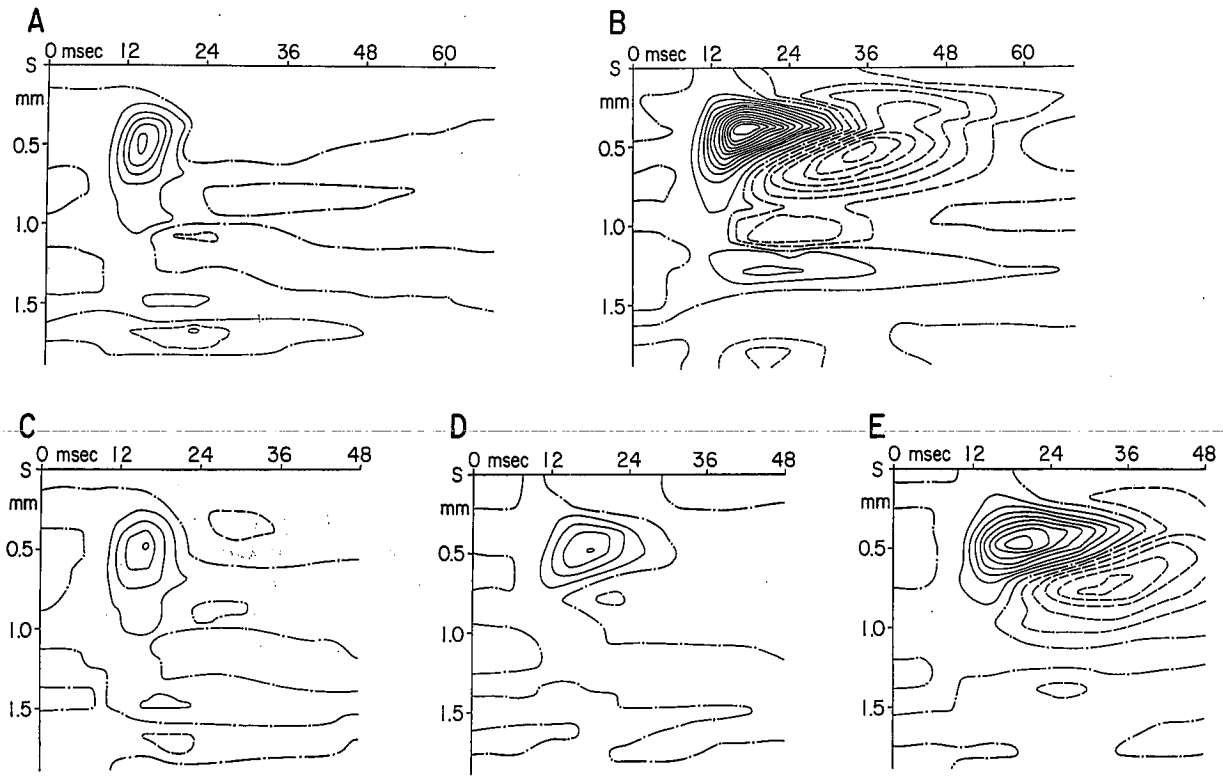

Fig. 5. A, C: current flow contour maps for responses to contralateral forepaw stimulation at 1/sec (A) and 3/sec (C) in normal cortex. B: current flow contour for responses to 1/sec stimulation in strychnine-treated cortex. D: contour map for 'small half' of the alternating series. Small and large halves constructed by grouping even- and odd-numbered responses in the series as shown in Fig. 2C and B. Contours are spaced at 50 $\mu A/cm^2$ intervals; $J_z > 0$ (upward current) dashed, and $J_z < 0$ (downward current) solid.

current flow in the depth interval $0.4 < z < 0.8$ mm, and in the associated weakening of the subsequent net upward current flow in layer II.

On the other hand, the pattern of J(z,t) made up from the 'large half' of the alternation series (Fig. 5E) was similar, at least in its upper half, to that associated with the 1/sec strychnine spike (Fig. 5B). Because both sets of measurements were taken during the same microelectrode penetration, the downward displacement of the current flow pattern by about 0.1 mm and the decrease in slope from 0.018 m/sec in Fig. 5B to 0.014 m/sec in Fig. 5E may be significant. Maximal current flow during the 'large half' of the alternation series was only 70% of that measured during the 1/sec strychnine spike. Possibly, some neurons failed to respond to the 4/sec stimulus: they may have been the more superficially located neurons of layer II. This would be consistent with our experience with the 'frequency-following' capabilities of untreated neurons isolated at different depths (Towe et al. 1968, 1976). The marked decrease of current flow in the lower half of the cortex during the alternation phenomenon may reflect a general failure of input to these deep-lying neurons, though we know of no precedent for such an interpretation. Nonetheless, the overall aspect of the two 'halves' of the alternation patterns is that of a somewhat enhanced normal pattern (Fig. 5D) and of a somewhat attenuated strychnine pattern (Fig. 5E).

Current source density patterns

It was argued in the Methods section that a single second derivative approach to estimating net transmembrane current flow should yield a sufficiently accurate picture. The resultant pattern, $i_m(z,t)$, when considered in relation to some model of synaptic connections within the tissue, would allow inferences about the depth-time loci of depolarizing (sinks) and hyperpolarizing (sources) synaptic actions. Fig. 6 illustrates the process: part 1 shows J(z,t), part 2 shows $i_m(z,t)$, and part 3 shows a three-dimensional display of $i_m(z,t)$, rotated about 50° counterclockwise. Column A of Fig. 6 shows the normal patterns during the primary evoked response and column B shows the patterns associated with the fully developed strychnine spike. In part 2, the time-depth contour lines of zero net transmembrane current flow, $i_m = 0$, are broken with dots; those of sources are solid and those of sinks are dashed. The contour lines are spaced at about 5 $\mu A/mm^3$ intervals. When taken in relation to the circuitry shown in Fig. $4B_1$, the source/sink couplet in the upper half of the tissue in the 11—15 msec interval in Fig. $6A_2$ would appear to reflect excitatory synaptic action onto *sa* neurons in the 0.4—0.8 mm depth interval (current *a* in Fig. 4B) due to thalamocortical afferent action. The subsequent sink/source couplet probably reflects the hyperpolarization that appears on the same *sa* neurons after the depolarizing response (Towe 1966; Whitehorn and Towe 1968); the probable circuitry underlying this event is not shown in Fig. $4B_1$. The sink/source couplets centering 1.0 mm and 1.4 mm below the pial surface probably reflect the predominantly excitatory synaptic actions of *sa* neurons onto *m* neurons (currents *k* and *c*, respectively, in Fig. 4B), the effects of the wide-field input pathway (input II in Fig. 4B) being considerably weaker.

The current source density picture after topical application of strychnine (Fig. $6B_2$) is a markedly intensified and prolonged version of the normal pattern (Fig. $6A_2$). The early, superficial source/sink couplet increases by a factor of 10 in total net transmembrane current, and the subsequent sink/source couplet shows a similar increase. The deeper sink/source couplets show only mild increases in intensity, but are markedly prolonged (consistent with the model of *sa* facilitation of *m* neurons) and show a 12 msec oscillation in intensity (with a lesser 4 msec oscillation not apparent in the source density maps presented). The overall net upward sweep of the sink through layers III and II proceeds at about 0.15 m/sec — similar to the apparent

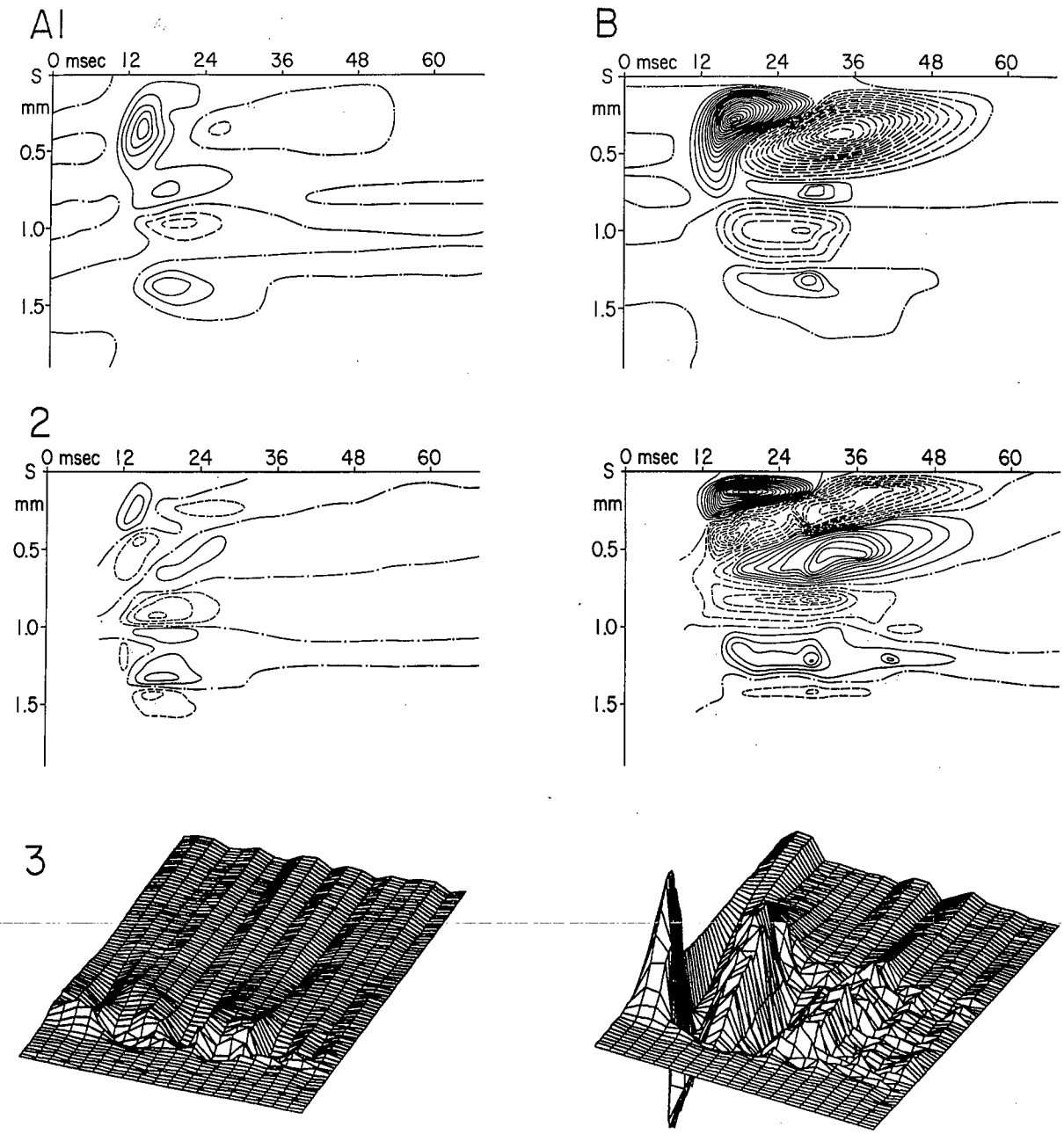

Fig. 6. Row 1: control (A_1) and strychnine (B_1) current flow contour maps for contralateral forepaw stimulation at 1/sec. Current source density (second-order difference) contours calculated from current flow contours in row 1 are shown in row 2 for normal (A_2) and strychnine-treated (B_2) cortex. Zero transmembrane currents ($i_m = 0$) are shown as broken lines with dots, contours for sources as solid lines, and those for sinks by dashed lines. The i_m contour lines are spaced at about 5 $\mu A/mm^3$ intervals. Three-dimensional displays of the transmembrane currents are shown in A_3 (corresponding to A_2) and B_3 (corresponding to B_2). Note that these are rotated 50° counterclockwise with respect to those in Fig. 3, row 3; time reads bottom to top (0—68 msec) and depth reads left to right in 0.1 mm intervals (first record corresponds to 0.1 mm). Sources are indicated by upward deflections, sinks by downward deflections.

upward velocity shown by the slopes of the iso-current contour lines in the lower row of Fig. 4. A striking feature, however, is that the source and sink depth-time 'domains,' as reflected in the positions of the $i_m = 0$ contour lines, are almost identical between the normal (Fig. $6A_2$) and strychnine (Fig. $6B_2$) patterns. This strongly suggests that the events that occur in the normal cerebral cortex also occur in the presence of strychnine. However, the normal source/sink couplet in the upper half of the cortex shows an apparent upward sweep of about 0.08 m/sec, close to the value discussed earlier. If this rapid event occurs in the presence of strychnine, it is obscured by the intense, slower event.

Calculation of current source density patterns for alternate responses during the strychnine alternation phenomenon (Fig. 7) showed the same features as found when net vertical current flow patterns were calculated (Fig. 5): the current source density patterns alternated between one akin to the normal pattern and one similar to the full strychnine pattern observed with 1/sec stimulation. The patterns fell short of these stated associations in that the 'small' alternate responses showed more intense transmembrane current flows than either the normal 1/sec or normal 3—4/sec values, whereas the 'large' alternate responses showed less intense i_m than the full strychnine response. Either the neurons do not alternate in perfect synchrony, or some fail to alternate, thus yielding smaller strychnine responses than at lower iterative stimulus rates. Overall, the observations are consistent with the idea that in the presence of strychnine, afferent input evokes a slightly enhanced 'normal'

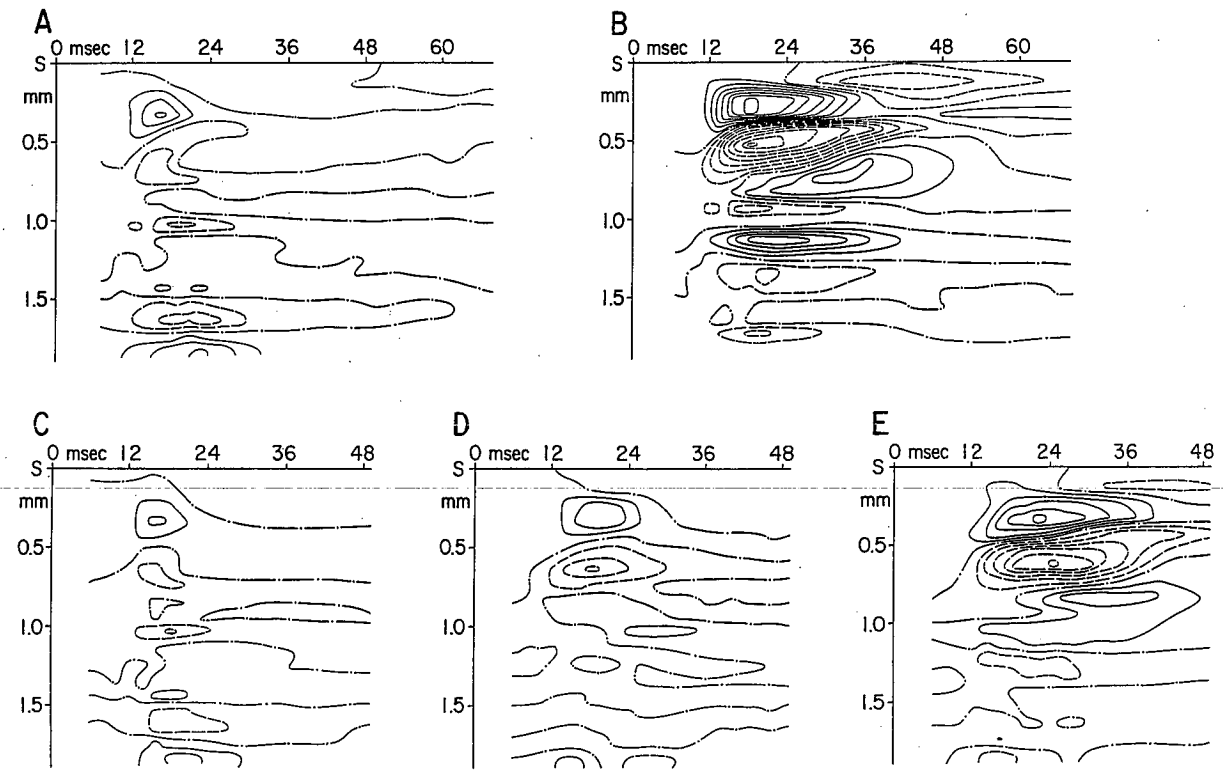

Fig. 7. Current source density contour plots computed for the data of Fig. 5 for responses to contralateral forepaw stimulation at 1/sec (A, B) and 3/sec (C—E), before (A, C) and after (B, D, E) strychnine treatment. Plots for both large (E) and small (D) alternate responses are shown. Conventions and calibrations as in Fig. 6, row 2.

event, with a new and independent process superimposed in the superficial half of the cortex.

Discussion

The response of pericruciate cerebral cortex to an afferent input changes continuously with time after topical application of strychnine sulfate. The strychnine 'spike' appears in less than 1 min, grows in amplitude over the next few minutes, maintains a plateau for 7—12 min, and gradually declines in amplitude over the next 30—45 min. Even during its plateau phase, there are slight changes in its configuration and in the duration of its positive and negative phases. The measurements in the present study were taken during the plateau phase, each complete run requiring 6—12 min.

In a general sense, the time-depth pattern of net vertical current flow derived during the fully developed strychnine 'spike' is a greatly enhanced, temporally extended version of the pattern derived during the normal primary response. The dominant feature in both cases is a large downward and lesser upward current flow in the upper half of the cortex; net vertical current flow in the lower half of the cortex is considerably smaller. As expected from studies of the surface gross potential (Towe and Mann 1973) and single neuron responses (Mann and Towe 1974) to stimulation of cutaneous sites not topographically related (off-focus) to the site of strychnine application, there was no change in the pattern or magnitude of current flow evoked by off-focus stimulation after topical application of strychnine to the posterior sigmoid gyrus. A more detailed examination of the data suggests that a new process develops during the strychnine 'spike' — one that is not involved in the normal primary response. It is likely that this new process is a paroxysmal depolarization shift (Matsumoto and Ajmone Marsan 1964), and that the latter is itself a calcium spike. The strychnine 'spike' would thus reflect the aggregate of such calcium spikes, along with normal or enhanced EPSPs, occurring on numerous neurons. The observations leading to this idea are outlined below.

It appears that topically applied strychnine (i) enhances a normal process and (ii) adds a new process to the cerebral response to on-focus skin stimulation, but (iii) has no effect on the cerebral response to off-focus skin stimulation. By subtracting the current flow during the pre-strychnine primary response from that during the strychnine 'spike,' the current added as a consequence of the strychnine treatment can be isolated. The pattern of this additional current appears to consist of two parts: (i) a temporally extended, 'normal' flow and (ii) a new and intense flow in layers II and III. The location of both the major sources and sinks in the upper half of the cortex, and the results of single neuron (Mann and Towe 1974) and simulation (Towe 1966) studies, point directly to the *sa* neurons of layers II and III as the source of this new and intense current flow. The nature of the alternation phenomenon suggests that the temporally extended, 'normal' pattern of current flow is gradable both with stimulus strength and iterative stimulus rate, whereas the new and intense current flow in layers II and III is all-or-none, with a fairly clear threshold and a long unresponsive period.

Calculation of transmembrane current flow shows the net source of 0.2—0.4 mm, and the net sink 0.4—0.6 mm, below the pial surface to be the first clear events to develop after on-focus cutaneous stimulation. The circuit model states that the sink is produced by thalamocortical input onto the deeper *sa* neurons, thus accounting for the early net downward current flow in layers II and III. The rapid upward spread of activity among *sa* neurons (Amassian et al. 1964; Towe et al. 1964, 1968; Towe 1966) may account for the apparent upward progression of the net sink. As the source/sink couplet dies away, a sink/source couplet develops just a little deeper and may be due to recurrent inhibitory action

among the *sa* neurons (Towe 1966; Whitehorn and Towe 1968; Satterthwaite et al. 1978), as well as a delayed potassium current (Barrett and Barrett 1976; Meech 1978; Moolenaar and Spector 1979), thus accounting for the later net upward current flow in layers II and III. Topical application of strychnine greatly enhances *both* of these source/sink couplets, and leads to a slow upward progression of the sink. The current flows deeper in the tissue can be ascribed to the deeper lying *m* neurons, and their enhancement following topical application of strychnine most probably results from the increased excitatory input from *sa* neurons rather than a direct action of strychnine on these neurons (Amassian et al. 1964; Towe 1966; Towe et al. 1968, 1976; Towe and Mann 1973; Mann and Towe 1974; Slimp and Towe 1980). Thus, the primary problem is to account for the greatly enhanced current flows driven by *sa* neurons after strychnine application.

Depolarization shift

In 1959, Li described a large, long-lasting decrease in membrane polarization on some intracellularly recorded neurons in strychnine-treated cerebral cortex. The spikes evoked by this depolarization decreased in amplitude or disappeared altogether during the maximal depolarization, but regained their former amplitude as the membrane repolarized. Pollen and colleagues (Pollen and Ajmone Marsan 1965; Pollen and Lux 1966) and Sawa et al. (1966) later confirmed these observations. A similar phenomenon occurs on cerebral neurons in association with the EEG paroxysmal discharges that develop after topical application of penicillin (Matsumoto 1964; Matsumoto and Ajmone Marsan 1964; Prince 1968; Matsumoto et al. 1969; Ayala and Vasconetto 1972; Courtney and Prince 1977). Matsumoto and Ajmone Marsan (1964) named this event the paroxysmal depolarization shift, or PDS. The PDS seems to be a general phenomenon, recordable from a variety of neurons under a variety of conditions. In cerebral neurons, it not only appears after topical penicillin or strychnine treatment, but also after topical application of cobalt (Schwartzkroin et al. 1977), after systemic injection of pentylenetetrazol (Sugaya et al. 1964), after production of local freeze lesions (Goldensohn and Purpura 1963), in association with the seizure activity induced by cerebral surface stimulation (Sawa et al. 1963), and in the untreated conjugate focus of penicillin-treated cerebral cortex (Schwartzkroin et al. 1975a). It has even been observed in neocortical slice preparations bathed in a penicillin-containing medium (Courtney and Prince 1977). Though under certain circumstances the PDS may show graded properties (Prince 1966), it is fundamentally an all-or-none phenomenon with a clear threshold (Matsumoto 1964). It has a long unresponsive period, shows an alternation phenomenon (Matsumoto and Ajmone Marsan 1964; Prince 1966) like that described here for the strychnine spike, and occurs on neuronal membrane that in other respects behaves as normal membrane (Matsumoto et al. 1969). The events giving rise to the intense current flows observed in the upper half of postcruciate cortex during the strychnine 'spike' are probably PDSs that develop on *sa* neurons in layers II and III.

Calcium spikes

Like the PDS, the Ca spike appears as a large, long-lasting decrease in membrane polarization; it is an all-or-none event with a clear threshold. Calcium spikes occur (or can be produced) on neuronal membranes, though the conditions for their production may not normally be present. Llinás and Hess (1976) have demonstrated the existence of TTX-resistant spikes in avian Purkinje cells, and Schwartzkroin and Slawsky (1977) have found TTX-resistant, Ca^{2+}- and Ba^{2+}-facilitated, Mn^{2+}-blocked spikes in pyramidal neurons of hippocampal slice preparations. Both are large, long-duration, apparently all-or-none events suggestive of the PDS. Using plausible values for the relevant parameters, Traub and Llinás (1979) modeled hippocampal pyramidal neurons, and found that a PDS-

like polarization change and associated Na spike discharges could be produced by increasing calcium conductance on proximal apical dendritic membrane. Traub (1979) used a similar model for pyramidal-shaped cerebral neurons, and again produced characteristic PDS configurations and Na spike discharges by increasing calcium conductance on the proximal half of the apical dendrite. It thus seems highly likely that the strong current flows observed in layers II and III during the strychnine 'spike' are produced by relatively synchronous PDS activity on *sa* neurons, and that each PDS is itself a Ca spike (Prince and Schwartzkroin 1978; Schwindt and Crill 1980).

The conditions for evoking a Ca spike are not entirely clear. Eckert and Lux (1976) examined the activation kinetics of the slow inward current in bursting pacemaker neurons of the snail *(Helix)* and found the rising phase to be considerably slower during small than during large depolarizations. The inward Ca^{2+} current must be sufficiently large to offset the K^+ current that develops as a consequence of the Ca^{2+}-dependent potassium conductance increase (Barrett and Barrett 1976; Meech 1978). A large, somewhat prolonged EPSP may be sufficient to yield this effect. The presence of anomalous rectification in the quasi-steady-state current voltage relationship of vertebrate neurons (Noebels and Pedley 1977; Schwindt and Crill 1977) assures a region of membrane instability if a sufficiently large inward current depresses the 'notch' in the I—V curve below the zero flow condition. If strychnine increases this 'notch,' as occurs with penicillin on cat motoneurons (Schwindt and Crill 1980), then bursting activity would be enhanced.

Production of the strychnine spike

The first sign of a strychnine spike appears 0.5—1.0 min after topical application (Towe and Mann 1973; Mann and Towe 1974), allowing little time for diffusion of these large molecules over any great distance. Similarly, the effects of topical bicuculline, in crystalline form, appear within a minute (Harris and Towe 1976). After 3 min of exposure to a topical 'infinite source' of penicillin, Noebels and Pedley (1977) found a steep concentration gradient, with about 50% in layer I, and 88% within 0.5 mm and 96% within 1.0 mm of the source. Using the time of appearance of the first spontaneous epileptiform discharge as a criterion, Willmore et al. (1978) found that topical ferric ions had penetrated only 32 ± 12 μm (4—12 min), and Butler et al. (1977) found that topical cobalt chloride was chiefly in layer I (75%), with a maximal penetration of 0.5 mm (19—31 min). These findings point clearly to layer I as the probable locus of the process that leads to convulsive activity. In postcruciate field 4γ, layer I is 0.2—0.3 mm thick, and the boundary between layers III and V is about 1.0 mm deep, so that even penicillin is effectively confined to the upper 3 layers (Noebels and Pedley 1977).

The process that occurs in layer I must lead to increased EPSPs in the lower half of layer III, and must not interfere with the normal upward spread of activity on progressively more superficial neurons. If some thalamocortical axons terminate in both layers III and I, and if antidromic activity occurs in the layer I terminals when activated in the presence of a convulsive substance, the synaptic action in layer III could be enhanced sufficiently to evoke Ca spikes. Though there are no compelling data, there is precedence for both postulates. In an EM study, Jones and Powell (1970) found terminal degeneration consistently present in the lower half of layer I following destruction of the 'ventral thalamic nucleus.' Studying the same tissue with light microscopy and smaller lesions, Hand and Morrison (1970) remarked that 'A few degenerating fibers could be seen proceeding radially through laminae III and II, and others were noted coursing tangentially in lamina I.' After thalamic VL lesions, Strick and Sterling (1974) found that 18% of the total terminal degeneration was in the upper third of layer I, and 66% was in layer III (though VL thala-

mocortical neurons do not carry the cutaneous input that activates this tissue but do project into this tissue).

The second postulate finds support in several observations. Using a crayfish nerve-muscle preparation, Futamachi and Prince (1975) determined the site of action of penicillin to be at the presynaptic terminal. Later, Noebels and Prince (1977), using an isolated rat phrenic nerve-hemidiaphragm preparation, showed that addition of penicillin to the bathing medium resulted in the appearance of a burst of antidromic spikes in the phrenic nerve after each orthodromic stimulus. Earlier, Gutnick and Prince (1972, 1974) had discovered that a burst of antidromic spikes appears in thalamic VPL in association with 'convulsive spikes' in the cortex, and Schwartzkroin et al. (1975b) found similar events in thalamic VL. Noebels and Prince (1977) review several possible ways in which this could occur.

The model envisaged here consists, then, of an afferent input from the thalamus which acts both in layer III and in layer I. The cerebral neurons are normally protected from too intense an input by the strong recurrent inhibitory action in the thalamus (Andersen and Sears 1964). This protective inhibitory mechanism can be bypassed through topical application of a convulsant substance, by producing repetitive discharges in the layer I terminals and axons, which travel antidromically to invade the layer III terminals, effectively increasing and prolonging the synaptic depolarization in layer III. This would produce a large increase in calcium conductance, thus generating the strong downward current followed by the strong upward current in layers II and III that characterize the strychnine convulsive 'spike.' Increasing the rate of stimulation leads to the alternation phenomenon, which can be understood as a failure of the Ca-spike mechanism on alternate trials, even though the enhanced presynaptic bombardment develops in response to each stimulus.

These events develop on layer II and III neurons (Mann and Towe 1974), which in turn affect the deeper lying corticofugal neurons (Towe 1966, 1968; Towe et al. 1968, 1976; Towe and Mann 1973; Mann and Towe 1974), increasing their output. When this synaptic bombardment becomes sufficiently intense, the same convulsive events may develop on these corticofugal neurons. Their evident interconnection (Towe et al. 1968, 1976; Towe and Tyner 1971; Slimp and Towe 1980), perhaps even through gap junctions (Sloper and Powell 1978a, b), offers the possibility of spread of convulsive activity into neighboring, normal tissue, in the extreme case involving the entire interconnected set. Spread to the opposite hemisphere might similarly occur. However, off-focus stimulation with respect to the potentially convulsive site does not lead to convulsive activity; the afferent cutaneous pathway to the corticofugal neurons may not possess thalamocortical layer I terminals. Nor do the various other pathways that affect these corticofugal neurons, such as visual, auditory, vestibular and visceral (see Slimp and Towe 1980), possess such layer I terminals. On the other hand, the behavior of these pathways suggests that they are normally weak in their influence (Baker et al. 1971) and that they do not incorporate a strong recurrent inhibitory mechanism. If this is true, then it should be possible to evoke convulsive activity on these corticofugal neurons by sufficiently strong and prolonged visual, auditory, vestibular, or visceral stimulation in otherwise apparently normal animals, especially if the state of arousal of the system is appropriate.

Convulsive activity might arise in a number of ways, both within the cortex and along the pathways leading to it, and it could involve different sets of neuronal elements, in some cases remaining focal and in others generalizing within an interconnected set or spreading along a distributed network. Systemic injection of strychnine should act primarily by removing the protective recurrent inhibition in the thalamus or elsewhere. Selective thalamic lesions, on the other hand, would not be likely to lead to convulsive activity, for the

inhibitory interneurons are physically intermingled with the thalamocortical projection neurons. There would be strong selective pressures against animals that develop protective inhibitory cells physically removed from the projection neurons; such animals would be open to vascular insults with devastating consequences.

It should be added, parenthetically, that the general mechanism proposed here might lead also to 'paroxysmal pain' if it involved the appropriate neurons.

Summary

Patterns of net vertical current flow and current source density during the normal primary evoked response and the strychnine spike induced by topical application were measured using single first-order and second-order differences of voltages occurring in depth and time in the cat's pericruciate cerebral cortex. Net vertical current flow during the primary response was dominated by a large downward current in layers II and III, 12—24 msec in time after a stimulus to the contralateral forepaw. Smaller, net upward currents occurred in layer V, 14—28 msec, and in layer II, 20—30 msec after the stimulus. Topical strychnine resulted in a pattern of net current flow that was an intensified and prolonged version of that for the normal evoked response. The great intensification occurred in layers II and III, with small changes occurring in layer V. No changes in the patterns of net vertical current flow during responses to stimulation of the other 3 paws were caused by strychnine. These patterns of current flow, and the changes that occurred in them after strychnine, can be understood in terms of the known synaptic interactions between sets of cortical neurons and the direct effect of strychnine on superficial, small receptive field neurons, with indirect involvement of deeper, large receptive field neurons. Current source density analysis showed a source/sink couplet in layers II and III, 11—15 msec after the contralateral forepaw stimulus. Sink/source couplets also were found at the same depth at 20—30 msec, and in layer V at 12—24 msec. The current source density pattern after strychnine was also an intensified and prolonged version of that occurring before strychnine, the greatest intensification being evident in layers II and III. Rates of ascent through the cortex of various components of the voltage, current, and source density patterns, and alternation of the strychnine spike with a near-normal primary response at stimulus rates of 3—4/sec, suggest that the strychnine spike results from two causes: (i) an enhancement of a normal process and (ii) the appearance of a new process. It is suggested that the former cause involves enlarged EPSPs, while the latter involves generation of Ca^{2+} spikes by the enlarged EPSPs. It is also suggested that the effect of strychnine and other topical convulsants is exerted on thalamocortical afferent fibers in layer I, setting up antidromic spikes that influence layer III neurons by collaterals of the same thalamocortical fibers into this layer, with upward spread into layer II.

Résumé

A propos des courants qui s'écoulent lors de la pointe strychninique

Les auteurs mesurent la distribution du flux du courant vertical total et la densité des sources de courant au cours de la réponse évoquée primaire normale et de la pointe strychninique induite par application topique à l'aide de simples différences de premier ordre et de second ordre des tensions, en fonction de la profondeur et du temps dans le cortex cérébral péri-crucié du chat. Le flux du courant vertical total au cours de la réponse primaire est dominé par un grand courant vers le bas dans les couches II et III, 12—24 msec après un stimulus donné à la patte antérieure controlatérale. Des courants totaux dirigés vers le haut, plus faibles, surviennent dans la couche V, 14—28 msec, et dans la couche II,

20—30 msec après le stimulus. La strychnine en application topique entraîne une distribution des flux de courant total qui est une version amplifiée et prolongée de celle de la réponse évoquée normale. L'intensification maximale se produit dans les couches II et III, avec des changements faibles dans la couche V. Aucun changement de distributions des flux de courant vertical total n'est provoqué par la strychnine dans les réponses à la stimulation des trois autres pattes. Ces distributions du flux de courant, et leur modification après strychnine, peuvent être comprises en terme d'interactions synaptiques connues entre des ensembles de neurones corticaux et l'effet direct de la strychnine sur de petits champs de neurones réceptifs superficiels, avec implication indirecte des champs de neurones plus profonds et réceptifs. L'analyse des densités des sources de courant montre un ensemble sources/puits dans les couches II et III, 11—15 msec après stimulation de la patte controlatérale. Des ensembles sources/puits sont également observés à la même profondeur à 20—30 msec, et dans la couche V, à 12—24 msec. Le pattern de densité de source de courant après strychnine est également une version intensifiée et prolongée de celui que l'on observe avant strychnine, la plus grande intensification s'observant dans les couches II et III. La vitesse d'établissement au travers du cortex des différentes composantes de la tension, du courant et de la densité de source, et l'alternance de la pointe strychninique avec une réponse primaire proche du normal pour des fréquences de stimulation de 3—4 c/sec suggèrent que la pointe strychninique résulte de 2 causes: (i) une augmentation du processus normal et (ii) l'apparition d'un nouveau processus. Les auteurs suggèrent que la première cause implique un EPSP plus grand, tandis que la seconde implique la génération de pointes Ca^{2+} par l'EPSP élargi. Il est également suggéré que l'effet de la strychnine et d'autres convulsivants topiques s'exerce sur les fibres afférentes thalamo-corticales de la couche I, entraînant des pointes antidromiques qui influencent les neurones de la couche III par les collatérales des mêmes fibres thalamo-corticales à l'intérieur de cette couche, qui diffusent vers le haut dans la couche II.

The authors are indebted to Hanna H. Atkins for preparation of the illustrations and manuscript, and to Rose M. Stogsdill for the programming of the three-dimensional hidden-line graphics.

References

Amassian, V.E., Waller, H.J. and Macy, Jr., J. Neural mechanism of the primary somatosensory evoked potential. Ann. N.Y. Acad. Sci., 1964, 112: 5—32.

Andersen, P. and Sears, T.A. The role of inhibition in the phasing of spontaneous thalamocortical discharge. J. Physiol. (Lond.), 1964, 173: 459—480.

Ayala, G.F. and Vasconetto, C. Role of recurrent excitatory pathways in epileptogenesis. Electroenceph. clin. Neurophysiol., 1972, 33: 96—98.

Baker, M.A., Tyner, C.F. and Towe, A.L. Observations on single neurons in the sigmoid gyri of awake nonparalyzed cats. Exp. Neurol., 1971, 32: 388—403.

Barrett, E.F. and Barrett, J.N. Separation of two voltage-sensitive potassium currents, and demonstration of a tetrodotoxin-resistant calcium current in frog motoneurones. J. Physiol. (Lond.), 1976, 255: 737—774.

Butler, A.B., Willmore, L.J., Fuller, P.M. and Bass, N.H. Cytochemical affinity of pyramidal cell dendrites for divalent cobalt during initiation and calcium-induced blockade of epileptiform discharge. Exp. Neurol., 1977, 56: 386—399.

Courtney, K.R. and Prince, D.A. Epileptogenesis in neocortical slices. Brain Res., 1977, 127: 191—196.

Eckert, R. and Lux, H.D. A voltage-sensitive persistent calcium conductance in neuronal somata of *Helix*. J. Physiol. (Lond.), 1976, 254: 120—151.

Futamachi, K.J. and Prince, D.A. Effect of penicillin on an excitatory synapse. Brain Res., 1975, 100: 589—597.

Goldensohn, E.S. and Purpura, D.P. Intracellular potentials of cortical neurons during focal epileptogenic discharges. Science, 1963, 139: 840—842.

Gutnick, M.J. and Prince, D.A. Thalamocortical relay neurons: antidromic invasion of spikes from a cortical epileptogenic focus. Science, 1972, 176: 424—426.

Gutnick, M.J. and Prince, D.A. Effects of projected cortical epileptiform discharges on neuronal activities in cat VPL. I. Interictal discharge. J. Neurophysiol., 1974, 37: 1310—1327.

Hand, P.J. and Morrison, A.R. Thalamocortical pro-

jections from the ventrobasal complex to somatic sensory areas I and II. Exp. Neurol., 1970, 26: 291—308.

Harding, G.W. and Towe, A.L. An automated on-line, real-time laboratory for single neuron studies. Comput. biomed. Res., 1976, 9: 471—501.

Harding, G.W., Stogsdill, R.M. and Towe, A.L. Relative effects of pentobarbital and chloralose on the responsiveness of neurons in sensorimotor cerebral cortex of the domestic cat. Neuroscience, 1979, 4: 369—378.

Harris, F.A. and Towe, A.L. Effects of topical bicuculline on primary evoked responses in pericruciate and precoronal cortex of the domestic cat. Exp. Neurol., 1976, 52: 227—241.

Hassler, R. und Muhs-Clement, K. Architektonischer Aufbau des sensomotorischen und parietalen Cortex der Katze. J. Hirnforsch., 1964, 6: 377—420.

Hoeltzell, P.B. and Dykes, R.W. Conductivity in the somatosensory cortex of the cat — evidence for cortical anisotropy. Brain Res., 1979, 177: 61—82.

Jones, E.G. and Powell, T.P.S. An electron microscopic study of the laminar pattern and mode of termination of afferent fibre pathways in the somatic sensory cortex of the cat. Phil. Trans. roy. Soc. Lond. B, 1970, 257: 45—62.

Li, C.-L. Cortical intracellular potentials and their responses to strychnine. J. Neurophysiol., 1959, 22: 436—450.

Llinás, R. and Hess, R. Tetrodotoxin-resistant dendritic spikes in avian Purkinje cells. Proc. nat. Acad. Sci. (Wash.), 1976, 73: 2520—2523.

Mann, M.D. Sets of neurons in somatic cerebral cortex of the cat and their ontogeny. Brain Res. Rev., 1979, 1: 3—45.

Mann, M.D. and Towe, A.L. Effect of strychnine on single neurons of the pericruciate cerebral cortex. Exp. Neurol., 1974, 42: 388—411.

Matsumoto, H. Intracellular events during the activation of cortical epileptiform discharges. Electroenceph. clin. Neurophysiol., 1964, 17: 294—307.

Matsumoto, H. and Ajmone Marsan, C. Cortical cellular phenomena in experimental epilepsy: interictal manifestations. Exp. Neurol., 1964, 9: 286—304.

Matsumoto, H., Ayala, G.F. and Gumnit, R.J. Neuronal behavior and triggering mechanism in cortical epileptic focus. J. Neurophysiol., 1969, 32: 688—703.

Meech, R.W. Calcium-dependent potassium activation in nervous tissues. Ann. Rev. Biophys. Bioengng, 1978, 7: 1—18.

Morse, R.W. A 10-channel data acquisition system compatible with the IBM-709 computer. Proc. 16th Ann. Conf. Eng. Med. Biol., 1963, 5: 136—137.

Nicholson, C. and Freeman, J.A. Theory of current source-density analysis and determination of conductivity tensor for anuran cerebellum. J. Neurophysiol., 1975, 38: 256—268.

Noebels, J.L. and Pedley, T.A. Anatomic localization of topically applied [^{14}C]penicillin during experimental focal epilepsy in cat neocortex. Brain Res., 1977, 125: 293—303.

Noebels, J.L. and Prince, D.A. Presynaptic origin of penicillin afterdischarges at mammalian nerve terminals. Brain Res., 1977, 138: 59—74.

Nyquist, J.K. and Towe, A.L. Neuronal activity evoked in cat precruciate cerebral cortex by cutaneous stimulation. Exp. Neurol., 1970, 29: 494—512.

Pollen, D.A. and Ajmone Marsan, C. Cortical inhibitory postsynaptic potentials and strychninization. J. Neurophysiol., 1965, 28: 342—358.

Pollen, D.A. and Lux, H.D. Conductance changes during inhibitory postsynaptic potentials in normal and strychninized cortical neurons. J. Neurophysiol., 1966, 29: 369—381.

Prince, D.A. Modification of focal cortical epileptogenic discharge by afferent influences. Epilepsia, 1966, 7: 181—201.

Prince, D.A. The depolarization shift in 'epileptic' neurons. Exp. Neurol., 1968, 21: 467—485.

Prince, D.A. and Schwartzkroin, P.A. Nonsynaptic mechanisms in epileptogenesis. In: N. Chalazonitis and M. Boisson (Eds.), Abnormal Neuronal Discharges. Raven, New York, 1978: 1—12.

Satterthwaite, W.R., Burnham, J.A. and Towe, A.L. Wide-field conditioning effects on small-field neurons in the posterior sigmoid gyrus of domestic cats. Exp. Neurol., 1978, 60: 603—613.

Sawa, M., Maruyama, N. and Kaji, S. Intracellular potential during electrically induced seizures. Electroenceph. clin. Neurophysiol., 1963, 15: 209—220.

Sawa, M., Maruyama, N., Kaji, S. and Nakamura, K. Action of strychnine to cortical neurons. Jap. J. Physiol., 1966, 16: 126—141.

Schwartzkroin, P.A. and Slawsky, M. Probable calcium spikes in hippocampal neurons. Brain Res., 1977, 135: 157—161.

Schwartzkroin, P.A., Futamachi, K.J., Noebels, J.L. and Prince, D.A. Transcallosal effects of a cortical epileptiform focus. Brain Res., 1975a, 99: 59—68.

Schwartzkroin, P.A., Mutani, R. and Prince, D.A. Orthodromic and antidromic effects of a cortical epileptiform focus on ventrolateral nucleus of the cat. J. Neurophysiol., 1975b, 38: 795—811.

Schwartzkroin, P.A., Shimada, Y. and Bromley, B. Recordings from cortical epileptogenic foci induced by cobalt iontophoresis. Exp. Neurol., 1977, 55: 353—367.

Schwindt, P. and Crill, W.E. A persistent negative resistance in cat lumbar motoneurons. Brain Res., 1977, 120: 173—178.

Schwindt, P. and Crill, W.E. Role of a persistent inward current in motoneuron bursting during

spinal seizures. J. Neurophysiol., 1980, 43: 1296—1318.

Slimp, J.C. and Towe, A.L. Effects of pudendal nerve stimulation on neurons in pericruciate cerebral cortex of male domestic cats. Exp. Neurol., 1980, 67: 181—204.

Sloper, J.J. and Powell, T.P.S. Dendro-dendritic and reciprocal synapses in the primate motor cortex. Proc. roy. Soc. Lond. B, 1978a, 203: 23—38.

Sloper, J.J. and Powell, T.P.S. Gap junctions between dendrites and somata of neurons in the primate sensori-motor cortex. Proc. roy. Soc. Lond. B, 1978b, 203: 39—47.

Strick, P.L. and Sterling, P. Synaptic termination of afferents from the ventrolateral nucleus of the thalamus in the cat motor cortex. A light and electron microscope study. J. comp. Neurol., 1974, 153: 77—106.

Sugaya, E., Goldring, S. and O'Leary, J.L. Intracellular potentials associated with direct cortical response and seizure discharge in cat. Electroenceph. clin. Neurophysiol., 1964, 17: 661—669.

Towe, A.L. On the nature of the primary evoked response. Exp. Neurol., 1966, 15: 113—139.

Towe, A.L. and Mann, M.D. Effect of strychnine on the primary evoked response and on the corticofugal reflex discharge. Exp. Neurol., 1973, 39: 395—413.

Towe, A.L. and Tyner, C.F. Cortical circuitry underlying the mixed receptive fields of certain pyramidal tract neurons. Exp. Neurol., 1971, 31: 239—257.

Towe, A.L., Patton, H.D. and Kennedy, T.T. Response properties of neurons in the pericruciate cortex of the cat following electrical stimulation of the appendages. Exp. Neurol., 1964, 10: 325—344.

Towe, A.L., Whitehorn, D. and Nyquist, J.K. Differential activity among wide-field neurons of the cat postcruciate cerebral cortex. Exp. Neurol., 1968, 20: 497—521.

Towe, A.L., Tyner, C.F. and Nyquist, J.K. Facilitatory and inhibitory modulation of wide-field neuron activity in postcruciate cerebral cortex of the domestic cat. Exp. Neurol., 1976, 50: 734—756.

Traub, R.D. Neocortical pyramidal cells: a model with dendritic calcium conductance reproduces repetitive firing and epileptic behavior. Brain Res., 1979, 173: 243—257.

Traub, R.D. and Llinás, R. Hippocampal pyramidal cells: significance of dendritic ionic conductances for neuronal function and epileptogenesis. J. Neurophysiol., 1979, 42: 476—496.

Tyner, C.F. The naming of neurons: applications of taxonomic theory to the study of cellular populations. Brain Behav. Evol., 1975, 12: 75—96.

Tyner, C.F. and Towe, A.L. Interhemispheric influences on sensorimotor neurons. Exp. Neurol., 1970, 28: 88—105.

Whitehorn, D. and Towe, A.L. Postsynaptic potential patterns evoked upon cells in sensorimotor cortex of cat by stimulation at the periphery. Exp. Neurol., 1968, 22: 222—242.

Willmore, L.J., Hurd, R.W. and Sypert, G.W. Epileptiform activity initiated by pial iontophoresis of ferrous and ferric chloride on rat cerebral cortex. Brain Res., 1978, 152: 406—410.